10.1515/tvsb-2017-0011
**Transactions of the VŠB – Technical University of Ostrava**
Civil Engineering Series, Vol. 17, No. 1, 2017
paper #11

**Juraj KRÁLIK**[1]

# PROBABILISTIC NONLINEAR ANALYSIS OF THE NPP HERMETIC COVER FAILURE DUE TO EXTREME PRESSURE AND TEMPERATURE

**Abstract**

This paper describes the probabilistic nonlinear analysis of the reactor cover under a high internal overpressure and temperature. The scenario of the hard accident in NPP and the methodology of the calculation of the fragility curve of the failure overpressure using the probabilistic safety assessment PSA 2 level is presented. The model and resistance uncertainties were taken into account in the response surface method (RSM).

**Keywords**

Nuclear Power Plant, Reactor cover, Nonlinearity, Fragility curve, PSA, RSM, ANSYS.

## 1 INTRODUCTION

After the accident of nuclear power plant (NPP) in Fukushimi the IAEA in Vienna adopted a large-scale project "Stress Tests of NPP", which defines new requirements for the verification of the safety and reliability of NPP under extreme effects of the internal and external environments and the technology accidents [3].

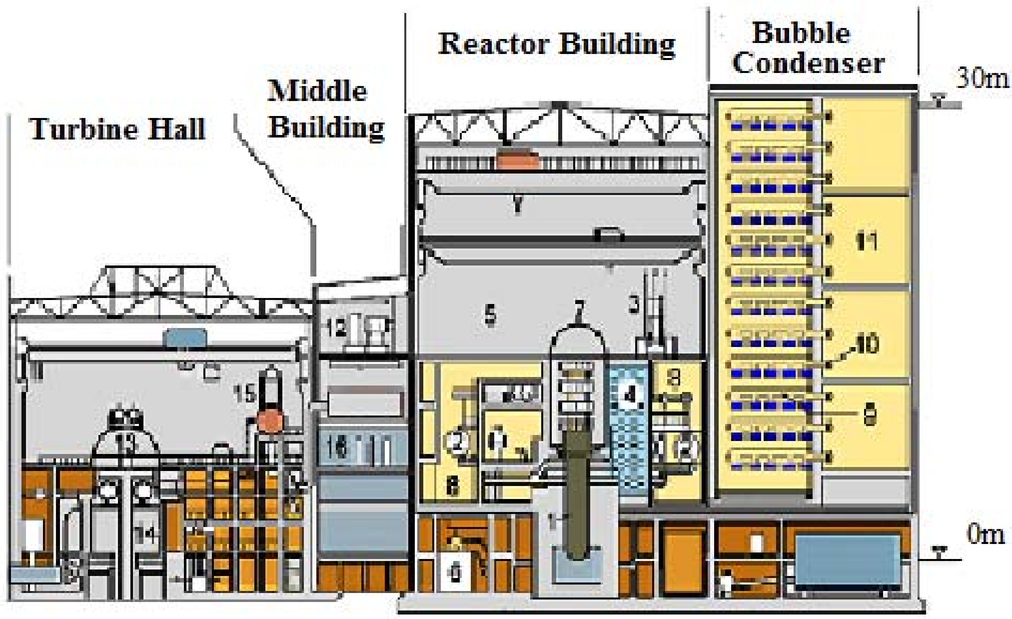


Fig.1: Section plane of the NPP with reactor VVER440/213

[1] Prof. Ing. Juraj Králik, CSc, Department of Structural Mechanics, Faculty of Civil Engineering, STU Bratislava, Radlinského 11, 810 05 Bratislava, e-mail: juraj.kralik@stuba.sk.

The experience from these activities will be used to develop a methodology in the frame of the project ALLEGRO, which is focused to the experimental research reactor of 4th generation with a fast neutron core. This project is a regional (V4 Group) project of European interest. The safety documents of NRC [18, 19] and IAEA [7] initiate the requirements to verify the hermetic structures of NPP loaded by two combinations of the extreme actions. A first extreme load is considered for the probability of exceedance $10^{-4}$ by year and second for $10^{-2}$ by year. Other action effects are considered as the characteristic loads during the accident. In the case of the loss-of-coolant accident (LOCA) the steam pressure expand from the reactor hall to the bubble condenser [12]. The reactor and the bubble condenser reinforced structures (see Fig.1) with steel liner are the critical structures of the NPP hermetic zone [14, 15]. Next, one from the critical technology structures is the reactor hermetic cover.

## 2 SCENARIO OF THE ACCIDENT

The previous analysis was achieved for the overpressure value of 100 kPa due to design basic accident (DBA), which corresponds of the loss of coolant accident due to guillotine cutting of the coolant pipe [12]. When the barbotage tower operates in the partial or zero performance the overpressure is equal to the 150-300 kPa. The ENEL propose the maximum temperature in the reactor shaft is equal about to 1800°C and in the containment around the reactor shaft is equal about to 350°C [15]. The possibility of the temperature increasing to the containment failure state is considered in the scenario too. In the case of the hard accident the overpressure can be increased linearly and the internal and external temperature are constant. Three types of the scenarios were considered (Tab.1).

Tab.1: The assumed scenarios of the accidents in the hermetic zone

| Type | Duration | Overpressure in HZ [kPa] | Extreme internal temperatures [°C] |
|---|---|---|---|
| I. | 1 hour – 1 day | 150 | 127 |
| II. | 2 hours – 7 days | 250 | 150 |
| III. | 1 year | - | 80-120 |

The critical was the accident during 7 days with the overpressure 250 kPa, internal temperature 150°C and external temperature -28°C.

## 3 CALCULATION MODEL

The technology segments of the NPP hermetic zone are made from the steel. The reactor protective hood is shown in Fig.2. The protective hood is an all-welded structure consisting of a spherical and a cylindrical part. The spherical part has a manhole of 500 mm in diameter with a ladder. The manhole facilitates equipment maintenance in the concrete cavity without the necessity to remove the protective hood. In order to ensure higher strength of the structure (on a seismic event), the protective hood is reinforced with a pipe (inner ∅712 mm) and 6 ribs. At the top, the pipe is welded in the center of the hood spherical part, while the other end covers the ring on the upper block beam. The protective hood is set on a counter - flange and is attached to it with sixty M48 bolts and sealed with packing. The cap structure includes a platform with railing.

The finite element model of reactor cover was created in software ANSYS by the shell, beam, combine and mass elements. The envelope of cover is from layered shell elements (SHELL181). The surface load is defined using 3D structural surface elements (SURF154). The connection with bolts is modelled by the combine elements (COMBINE14). The element of point mass (MASS21) present the concentrated masses adequate to local load of the technology, beam elements (BEAM44) for frame and beam connection.

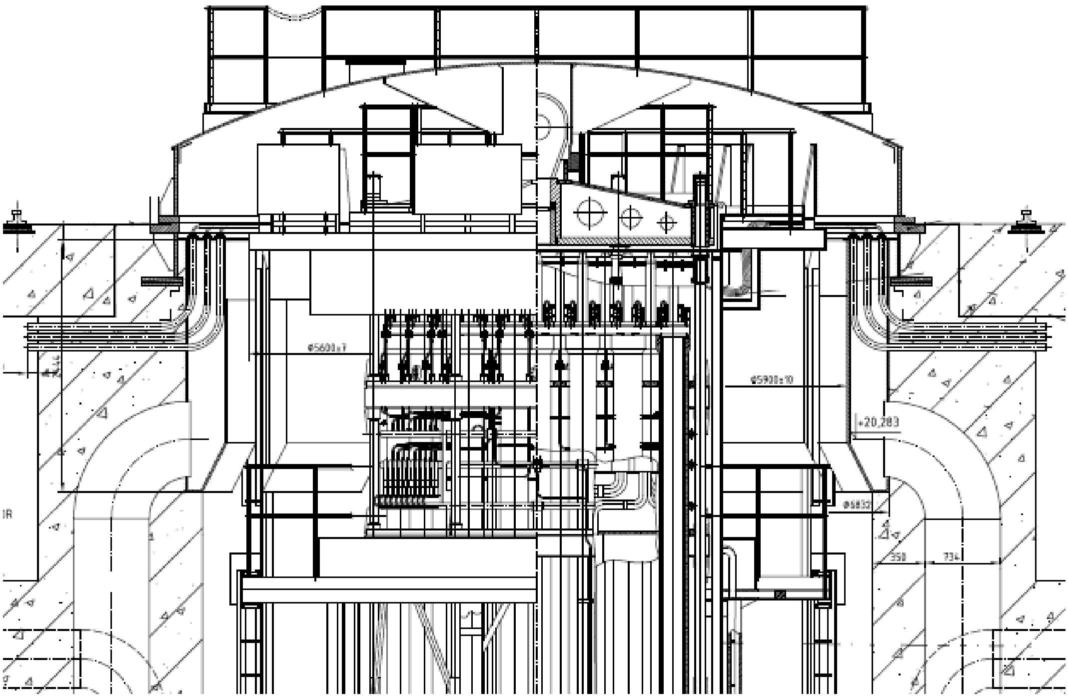


Fig.2: Vertical section of the reactor with reactor protective hood

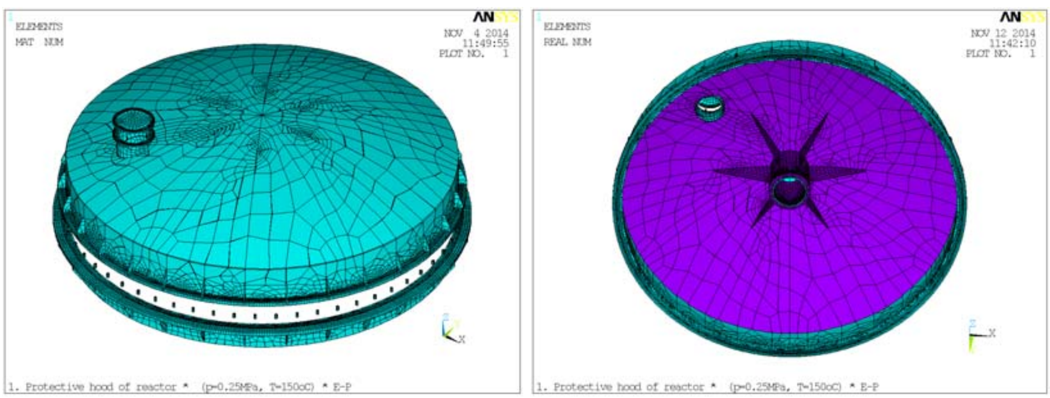


Fig.3: FEM model (RCOV) of the reactor protective hood

The contact element (CE) and links (CP) were used for the joint connection. The upper part of the hood has lugs used to handle it. The FEM model (RCOV) consists 27824 shell, beam and mass elements with 22887 nodes (Fig.3).

## 4 ACCEPTANCE CRITERIA

In the case of the nonlinear analysis the thermal depended material properties are used following the input data for material 08CH18N10T defined in standard CSN 413240, CSN 411700, CSN 413230, CSN 413240 and NTD SAI Section II [1]. The criterion for the max. stress values are limited by the HMH plastic potential [1, 10, 12]. The failure of the steel structure is limited by the max. strain values or by the stability of the nonlinear solution [12].

The standard STN EN 1993 1-2 [6] define following characteristic values of the strain for the structural steel:

- yield strain $\varepsilon_{ay,\theta} = 0.02$
- ultimate strain $\varepsilon_{au,\theta} = 0.15$
- max. limit strain $\varepsilon_{ae,\theta} = 0.20$

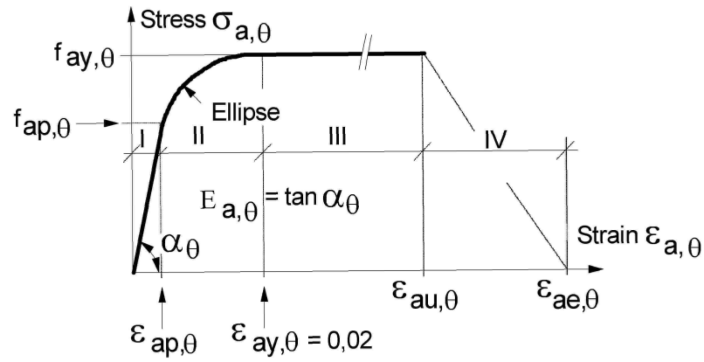


Fig.4: Stress-strain relationship of the steel dependent on temperature [6]

The stress-strain relationship for the steel (Fig.4) are considered in accordance of Eurocode [6] on dependency of temperature level for heating rates between 2 and 50 K/min. In the case of the steel the stress-strain diagram is divided on four regions.

The stress-strain relations $\sigma_{a,\theta} \approx \varepsilon_{a,\theta}$ are defined in following form in region I:

$$\sigma_{a,\theta} = E_{a,\theta}\varepsilon_{a,\theta}, \qquad E_{a,\theta} = k_{E,\theta}E_a \tag{1}$$

where the reduction factor can be chosen according to Eurocode [6]

In region II:

$$\sigma_{a,\theta} = \left(f_{ay} - c\right) + \frac{b}{a}\sqrt{a^2 - \left(\varepsilon_{ay,\theta} - \varepsilon_{a,\theta}\right)^2}, \qquad a^2 = \left(\varepsilon_{ay,\theta} - \varepsilon_{ap,\theta}\right)\left(\varepsilon_{ay,\theta} - \varepsilon_{ap,\theta} + c/E_{a,\theta}\right)$$

$$b^2 = E_{a,\theta}\left(\varepsilon_{ay,\theta} - \varepsilon_{ap,\theta}\right)c + c^2, \qquad c = \frac{\left(f_{ay,\theta} - f_{ap,\theta}\right)^2}{E_{a,\theta}\left(\varepsilon_{ay,\theta} - \varepsilon_{ap,\theta}\right) - 2\left(f_{ay,\theta} - f_{ap,\theta}\right)} \tag{2}$$

and in region III:

$$\sigma_{a,\theta} = f_{ay,\theta} \tag{3}$$

## 5 NONLINEAR ANALYSIS

The nonlinear analysis based on potential theory considering the isotropic material properties was made for the layered shell elements SHELL181 in the FEM model.

The steel is typical isotropic material. The elastic-plastic behavior of the isotropic materials is described by the HMH yield criterion.

Consequently the stress-strain relations are obtained from the following relations

$$\{d\sigma\} = [D_{el}]\left(\{d\varepsilon\} - \{d\varepsilon^{pl}\}\right) = [D_{el}]\left(\{d\varepsilon\} - d\lambda\left\{\frac{\partial Q}{\partial\sigma}\right\}\right) \tag{4}$$

or

$$\{d\sigma\} = \left[D_{ep}\right]\{d\varepsilon\} \tag{5}$$

where $\left[D_{ep}\right]$ is elastic-plastic matrix in the form

$$\left[D_{ep}\right] = [D_e] - \frac{[D_e]\left\{\frac{\partial Q}{\partial\sigma}\right\}\left\{\frac{\partial F}{\partial\sigma}\right\}^T [D_e]}{A + \left\{\frac{\partial F}{\partial\sigma}\right\}^T [D_e]\left\{\frac{\partial Q}{\partial\sigma}\right\}} \tag{6}$$

The hardening parameter *A* depends on the yield function and model of hardening (isotropic or kinematic). Huber-Mises-Hencky (HMH) define the yield function in the form

$$\sigma_{eq} = \sigma_T\left(\kappa\right), \tag{7}$$

where $\sigma_{eq}$ is equivalent stress in the point and $\sigma_o\left(\kappa\right)$ is yield stress depends on the hardening.

In the case of kinematic hardening by Prager (versus Ziegler) and the ideal Bauschinger's effect is given

$$A = \frac{2}{9E}\sigma_T^2 H' \tag{8}$$

The hardening modulus *H'* for this material is defined in the form

$$H' = \frac{d\sigma_{eq}}{d\varepsilon_{eq}^p} = \frac{d\sigma_T}{d\varepsilon_{eq}^p} \tag{9}$$

When this criterion is used with the isotropic hardening option, the yield function is given by:

$$F(\sigma) = \sqrt{\{\sigma\}^T [M]\{\sigma\}} - \sigma_o\left(\varepsilon_{ep}\right) = 0 \tag{10}$$

where $\sigma_o\left(\varepsilon_{ep}\right)$ is the reference yield stress, $\varepsilon_{ep}$ is the equivalent plastic strain and the matrix [*M*] is as follows

$$[M] = \begin{bmatrix} 1 & 0 & 0 & 0 & 0 & 0 \\ 0 & 1 & 0 & 0 & 0 & 0 \\ 0 & 0 & 1 & 0 & 0 & 0 \\ 0 & 0 & 0 & 2 & 0 & 0 \\ 0 & 0 & 0 & 0 & 2 & 0 \\ 0 & 0 & 0 & 0 & 0 & 2 \end{bmatrix} \tag{11}$$

Tab.2: Extreme stress-strain values of the reactor protective hood for the accident scenario type II

| Node | $\varepsilon_1$ | $\varepsilon_2$ | $\varepsilon_3$ | $\varepsilon_{\text{int}}$ | $\varepsilon_{eqv}$ |
|---|---|---|---|---|---|
| Minimum Values of Strain | | | | | |
| Node | 15981 | 4867 | 5041 | 7922 | 2008 |
| Value | 0.50974E-07 | -0.43109E-03 | -0.13648E-02 | 0.19194E-06 | 0.17439E-06 |
| | | | | | |
| Maximum Values of Strain | | | | | |
| Node | 12581 | 6169 | 7928 | 5041 | 13890 |
| Value | 0.10619E-02 | 0.27617E-03 | -0.68012E-07 | 0.0020612 | 0.0018831 |
| | | | | | |
| Node | $\sigma_1$ | $\sigma_2$ | $\sigma_3$ | $\sigma_{\text{int}}$ | $\sigma_{eqv}$ |
| Minimum Values of Stress [MPa] | | | | | |
| Node | 6003 | 5251 | 6177 | 7922 | 7922 |
| Value | -38.650 | -122.29 | -212.96 | 0.028264 | 0.024501 |
| | | | | | |
| Maximum Values of Stress [MPa] | | | | | |
| Node | 12581 | 22512 | 1588 | 6177 | 12581 |
| Value | 198.88 | 65.451 | 17.063 | 212.92 | 200.43 |

On the base of the elastic-plastic theory and the HMH function of plasticity the extreme strain and stress of the reactor cover for the accident scenario type II are presented in the Table 2.

## 5 PROBABILITY NONLINEAR ASSESSMENT OF THE ACCIDENT

The probabilistic methods are very effective to analyse of the safety and reliability of the structures considering the uncertainties of the input data [2, 4-18, 20, 21 and 22]. The probability analysis of the loss of the reactor cover integrity was made for the overpressure loads from 250 kPa to 1000 kPa using the nonlinear solution of the static equilibrium considering the geometric and material nonlinearities of the steel shell and beam elements. The probability nonlinear analysis of the technology segments is based on the proposition that the relation between the input and output data can be approximated by the approximation function in the form of the polynomial [12, 13]. The full probabilistic assessment was used to get the probability of technology segment failure. The safety of the technology segments was determined by the safety function *SF* in the form [5]

$$SF = E/R \qquad \text{and} \qquad 0 \le SF < 1 \tag{12}$$

where *E* is the action function and *R* is the resistance function.

The reliability function *RF* is defined in the form

$$RF = g\left(R,E\right) = 1 - SF = R - E > 0 \tag{13}$$

where $g\left(R,E\right)$ is the reliability function.

The probability of failure can be defined by the simple expression

$$P_f = P\left[R < E\right] = P\left[\left(R - E\right) < 0\right] \tag{14}$$

The reliability function *RF* can be expressed generally as a function of the stochastic parameters $X_1$, $X_2$ to $X_n$, used in the calculation of *R* and *E*.

$$RF = g(X_1, X_2, ..., X_n) \tag{15}$$

The failure function $g(\{X\})$ represents the condition (capacity margin) of the reliability, which can be either an explicit or implicit function of the stochastic parameters and can be single (defined on one cross-section) or complex (defined on several cross-sections, e.g., on a complex finite element model).

In the case of the nonlinear analysis the correct solution of the elastic-plastic behaviour of the structures is determined by the function plasticity. The HMH function of the plasticity was used for the nonlinear solution of the steel technology segments. This plasticity function is defined in the form

$$R = f_y \quad \text{and} \quad E = \sigma_{ef}\,, \tag{16}$$

where the effective stress $\sigma_{ef}$ (Von Mises stress) is defined as follows

$$\sigma_{ef} = \left(\frac{1}{2}\left[(\sigma_1 - \sigma_2)^2 + (\sigma_2 - \sigma_1)^2 + (\sigma_3 - \sigma_1)^2\right]\right)^{\frac{1}{2}}, \tag{17}$$

The failure of the steel technology segments in the frame of the PSA analysis is defined by the ultilimite values of the maximal strain deformation. This failure function is defined in the form

$$R = \varepsilon_{a\,y,\theta} \quad \text{and} \quad E = \varepsilon_{ef}\,, \tag{18}$$

where the effective strain $\varepsilon_{ef}$ (Von Mises strain) is defined as follows

$$\varepsilon_{ef} = \frac{1}{1+\nu'}\left(\frac{1}{2}\left[(\varepsilon_1 - \varepsilon_2)^2 + (\varepsilon_2 - \varepsilon_1)^2 + (\varepsilon_3 - \varepsilon_1)^2\right]\right)^{\frac{1}{2}}, \tag{19}$$

where $\nu'$ is the effective Poisson constant.

The failure probability is calculated from the evaluation of the statistical parameters and theoretical model of the probability distribution of the reliability function $Z = g(X)$ using the simulation methods. The failure probability is defined as the best estimation on the base of numerical simulations in the form

$$p_f = \frac{1}{N}\sum_{i=1}^{N} I\left[g(X_i) \le 0\right] \tag{20}$$

where $N$ in the number of simulations, $g(.)$ is the failure function, $I[.]$ is the function with value 1, if the condition in the square bracket is fulfilled, otherwise is equal 0.

The full probabilistic method result from the nonlinear analysis of the series simulated cases considered the uncertainties of the input data.

The various simulation methods (direct, modified or approximation methods) can be used for the consideration of the influences of the uncertainty of the input data [13].

In case of the nonlinear analysis of the full FEM model the approximation method RSM (Response surface method) is the most effective method [13].

The RSM method is based on the assumption that it is possible to define the dependency between the variable input and the output data through the approximation functions in the following form:

$$Y = c_o + \sum_{i=1}^{N} c_i X_i + \sum_{i=1}^{N} c_{ii} X_i^2 + \sum_{i=1}^{N-1}\sum_{j>i}^{N} c_{ij} X_i X_j \tag{21}$$

where $c_o$ is the index of the constant member; $c_i$ are the indices of the linear member and $c_{ij}$ the indices of the quadratic member, which are given for predetermined schemes for the optimal distribution of the variables or for using the regression analysis after calculating the response.

Approximate polynomial coefficients are given from the condition of the error minimum, usually by the "Central Composite Design Sampling" (CCD) method or the "Box-Behnken Matrix Sampling" (BBM) method [10].

The computation efficiency of the experimental design depends on the number of design points, which must be at least equal to the number of the unknown coefficients. In the classical design approach, a regression analysis is carried out to formulate the response surface after calculating the responses at the sampling points. These points should have at least 3 levels for each variable to fit the second-order polynomial, leading to $3k$ factorial design. This design approach becomes inefficient with the increasing of the number of random variables. More efficient is the central composite design, which was developed by Box and Wilson [10].

The central CCD method is composed of (Fig.5):

1. Factorial portion of design - a complete $2k$ factorial design (equal -1, +1)
2. Center point - $n_o$ center points, $n_o \geq 1$ (generally $n_o = 1$)
3. Axial portion of design - two points on the axis of each design variable at distance $\alpha$ from the design center.

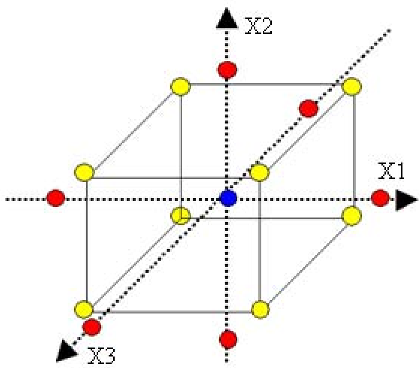


Fig.5: Distribution schemes of CCD for 3 input data

Then the total number of design points is $N = 2^k + 2k + n_o$, which is much more than the number of the coefficients $p = (k+1)(k+2)/2$.

The true performance function $g(\{X\})$ or $\{Y\}$ in Equation (21) can be represented in the matrix form as

$$\{Y\} = [X]\{c\} + \{\varepsilon\} \tag{22}$$

where $\{Y\}$ is the vector of actual responses, and $[X]$ is the matrix of the combination coefficients.

The least squares estimates $\{\hat{c}\}$, defined as $c_o$, $c_i$, $c_{ii}$ and $c_{ij}$ in Equation (22), are obtained by solution of the least square (regression) analysis, i.e.,

$$\{\hat{c}\} = \left([X]^T [X]\right)^{-1} [X]^T \{Y\} \tag{23}$$

The design includes several statistical properties such as orthogonality that makes the calculation of $[X]^T[X]$ term simple and rotability that insures the uniform precision of the predicted value.

The statistical postprocessor compiles the results numerically and graphically in the form of histograms and cumulative distributional functions. The sensibility postprocessor processes the data numerically and graphically and provides information about the sensitivity of the variables and about the correlation matrices.

On base of experimental design, the unknown coefficients are determined due to the random variables selected within the experimental region. The uncertainty in the random variables can be defined in the model by varying in the arbitrary amount producing the whole experimental region.

The total vector of the deformation parameters $\{r_s\}$ in the FEM is defined for the $s^{th}$-simulation in the form

$$\{r_s\} = \left[K_{GN}\left(E_s, F_\sigma\right)\right]^{-1}\left\{F\left(G_s, Q_s, P_s, T_s\right)\right\} \tag{24}$$

and the strain vector

$$\{\varepsilon_s\} = [B_s]\{r_s\} \tag{25}$$

where $[K_{GN}]$ is the nonlinear stiffness matrix depending on the variable parameters $E_s$ and $F_\sigma$, $F\sigma$ is the HMH yield function defined in the stress components, $\{F\}$ is the vector of the general forces depending on the variable parameters $G_s$, $Q_s$, $P_s$ and $T_s$ for the $s^{th}$-simulation.

## 6 UNCERTAINTIES OF THE INPUT DATA

The uncertainties are coming from the following sources [7, 8, 12, 13, 14, 18 and 19]:

- Parameters of material properties. Based on experiments with concrete elements the standard deviation is 11.1%. In case of other materials this value is about 5%.
- Assessment of mechanical characteristics error factors are about 8-12%, it depends on the construction material differences used for the different units with VVER 440/213. In some cases it can be conservative, in other cases non-conservative impact.
- Uncertainties in the numerical results in the value of 10-15%. In this area we can take into consideration the steel liner with the concrete elements.
- Uncertainties arising from the temperatures impact in the value of 10%.
- Other calculations assumptions 3-5%.

Tab.3: Variability of input parameters

| Quantity | Charact. value | Variable | Histog. type | Mean μ | Deviat. σ [%] | Minim. value | Maxim. value |
|---|---|---|---|---|---|---|---|
| Material | | | | | | | |
| Strength | $F_k$ | $f_{var}$ | N | 1.1 | 6.6 | 0.774 | 1.346 |
| Action effects | | | | | | | |
| Dead load | $G_k$ | $g_{var}$ | N | 1 | 5 | 0.808 | 1.195 |
| Pressure LOCA | $p_k$ | $p_{var}$ | N | 1 | 8 | 0.698 | 1.333 |
| Temperature | $T_k$ | $t_{var}$ | GU | 0.667 | 14.2 | 0.402 | 1.147 |
| Model uncertainties | | | | | | | |
| Action | $E_k$ | $e_{var}$ | N | 1 | 5 | 0.813 | 1.190 |
| Resistance | $R_k$ | $r_{var}$ | N | 1 | 5 | 0.812 | 1.201 |

The mean values and standard deviations were defined in accordance of the experimental test and design values of the material properties and the action effects [6 and 8] (see Tab.3). Based on the results from the simulated nonlinear analysis of the technology segments and the variability of the input parameters $10^6$ Monte Carlo simulations were performed in the system ANSYS [10].

## 7 PROBABILITY AND SENSITIVITY NONLINEAR ANALYSIS OF THE REACTOR COVER

The calculation of the probability of the reactor cover failure is based on the results of the nonlinear analysis for various level of the accident pressure and mean values of the material properties. The critical area of the technology segments defined from the nonlinear deterministic analysis is the mechanical closures. The CCD method of the RSM approximation is based on 45 nonlinear simulations depending on the 6 variable input data. The nonlinear solution for the one simulation consists about the 50 to 150 iteration depending on the scope of the plastic deformations in the calculated structures. The sensitivity analyses give us the informations about the influences of the variable properties of the input data to the output data (see Figs.6-9). These analyses are based on the correlations matrixes.

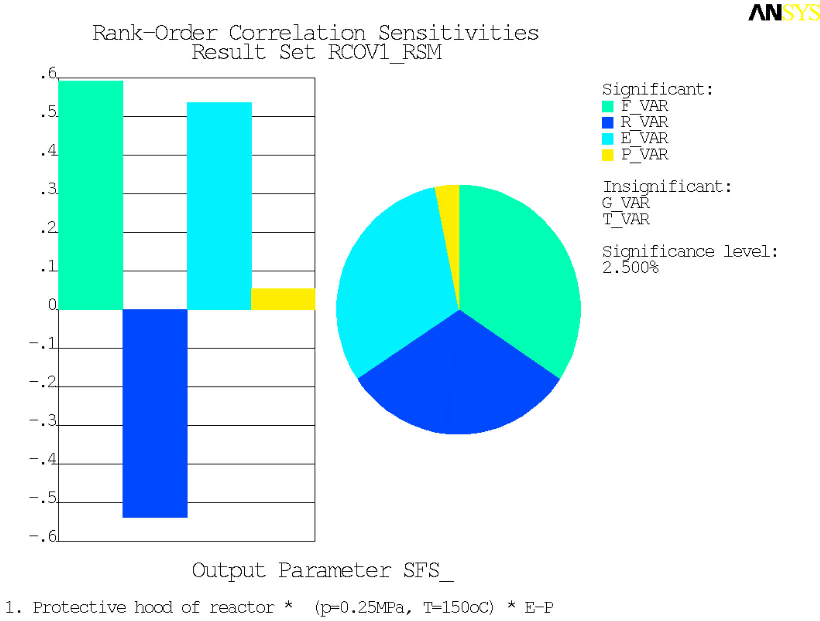


Fig.6: Sensitivity analysis of the safety function of the Reactor protective hood for overpressure $\Delta p = 0.25$ MPa

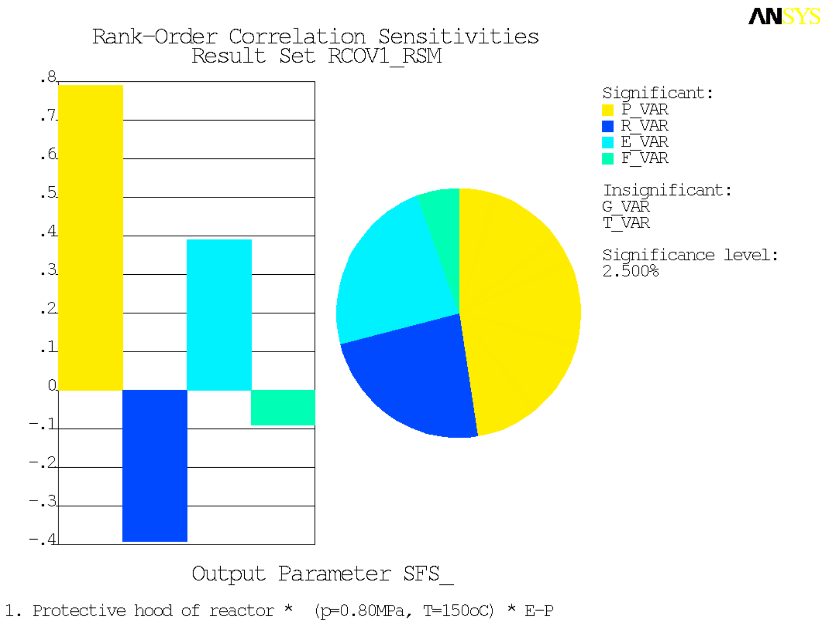


Fig.7: Sensitivity analysis of the safety function of the Reactor protective hood for overpressure $\Delta p = 0.80$ MPa

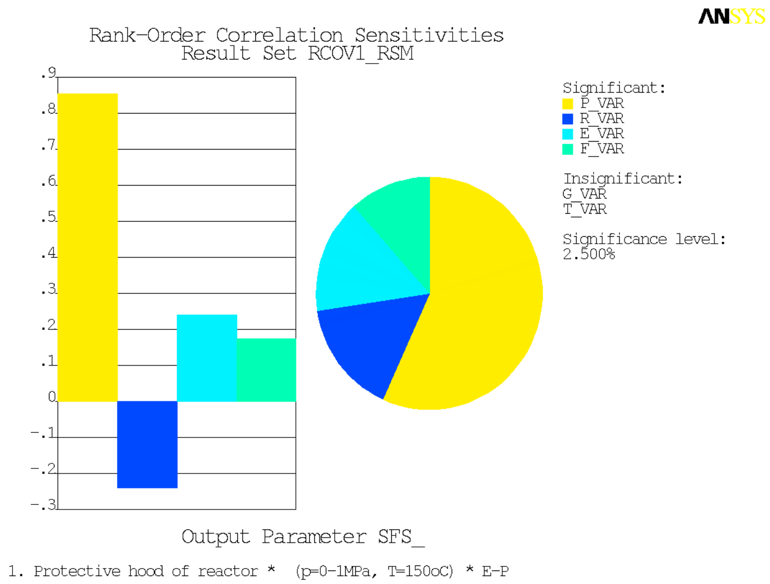


Fig.8: Sensitivity analysis of the safety function of the reactor cover for uniform distribution of overpressure

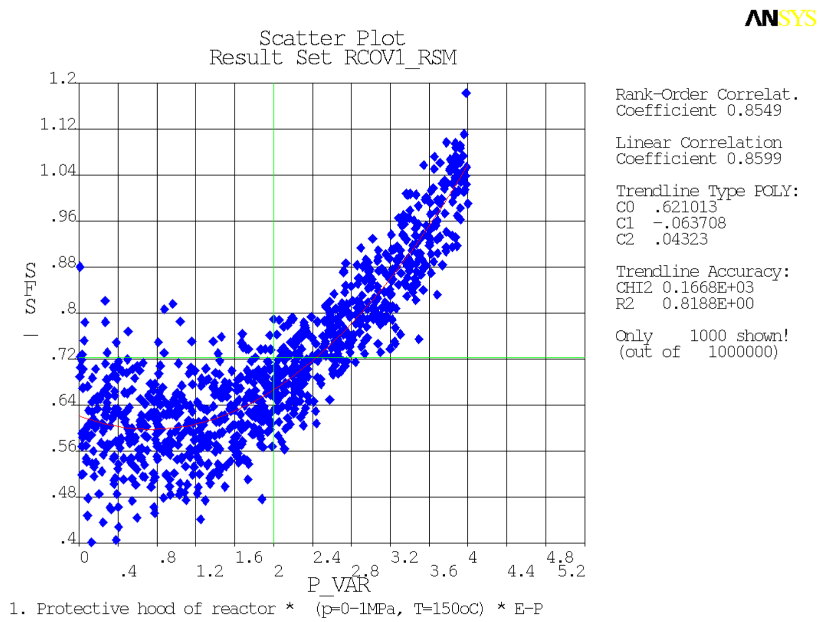


Fig.9: Trend analysis of the safety function of the reactor cover for uniform distribution of overpressure

## 8 FRAGILITY CURVES OF FAILURE PRESSURE

The PSA approach to the evaluation of probabilistic pressure capacity involves limit state analyses [5 and 12]. The limit states should represent possible failure modes of the confinement functions. Containment may fail at different locations under different failure modes (see Fig.10). Consider two failure modes A and B, each with *n* fragility curves and respective probabilities $p_i$ ($i$ = 1,…,$n$) and $q_j$ ($j$ = 1,…,$n$). Then the union $C$=$A$∪$B$, the fragility $F_{Cij}(x)$ is given by

$$F_{Cij}(x) = F_{Ai}(x) + F_{Bj}(x) - F_{Ai}(x)\,\mathrm{I}\,\, F_{Bj}(x) \tag{26}$$

where the subscripts *i* and *j* indicate one of the n fragility curves for the failure modes and x denote a specific value of the pressure within the containment. The probability $p_{ij}$ associated with fragility curve $F_{Cij}(x)$ is given by $p_i.\ q_j$ if the median capacities of the failure modes are independent. The result of the intersection term in (32) is $F_{Aj}(x).F_{Bj}(x)$ when the randomness in the failure mode capacities is independent and min[$F_{Ai}(x)$, $F_{Bj}(x)$] when the failure modes are perfectly dependent.

The following is and the consequence of an accident depends on the total leak area. Multiple leaks at different locations of the containment (e.g. bellows, hatch, and airlock) may contribute to the total leak area. Using the methodology described above, we can obtain the fragility curves for leak at each location (see Fig.10).

For a given accident sequence, the induced accident pressure probability distribution, *h(x)*, is known. This is convolved with the fragility curve for each leak location to obtain the probability of leak from that location ($P_{Li}$). It is understood that there is no break or containment rupture at this pressure.

$$p_{Li} = \int_0^\infty h(x)\left[1 - F_b(x)\right] F_l(x)\, dx\,, \tag{27}$$

where the $F_b(x)$ is the fragility of break at the location and $F_l(x)$ is the fragility of leak. The leak is for each location specified as a random variable with a probability distribution.

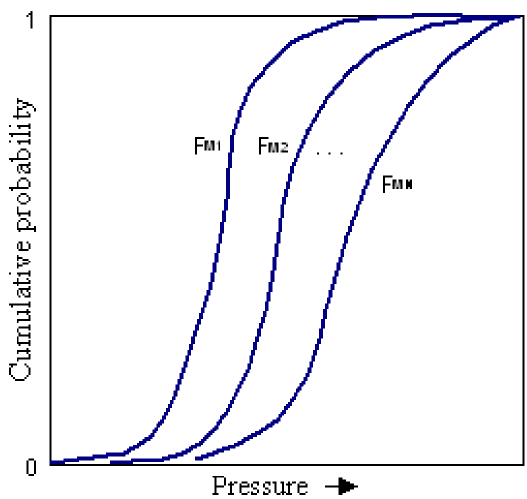


Fig.10: Family of fragility curves showing modelling uncertainty

The probability of reactor cover failure is calculated from the probability of the reliability function *RF* in the form,

$$P_f = P\,(RF < 0) \tag{28}$$

where the reliability condition *RF* is defined depending on a concrete failure condition

$$RF = 1 - \varepsilon_{ef} / \varepsilon_{ay,\theta}\,, \tag{29}$$

where the failure function was considered in the form (18).

The fragility curve of the failure pressure was determined using 45 probabilistic simulations using the RSM approximation method with the experimental design CCD for $10^6$ Monte Carlo simulations for each model and 5 level of the overpressure. The various probabilistic calculations for 5 constant level of overpressure next for the variable overpressure for gauss and uniform distribution were taken out.

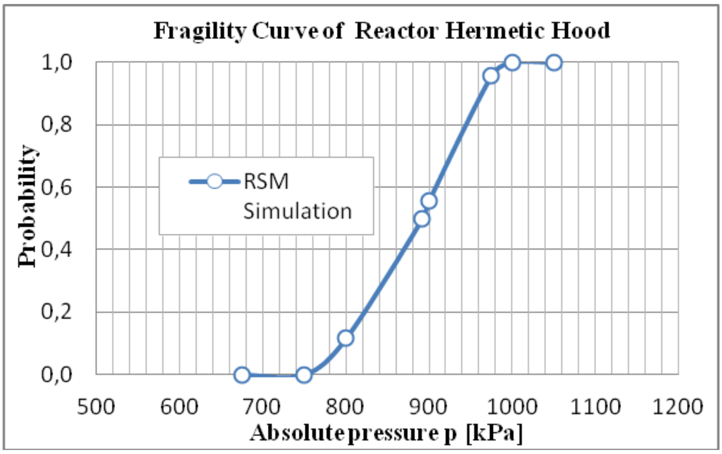


Fig.11: Fragility curve of the reactor protective hood determined by approximation method a RSM with CCD experimental design

The failure criterion of the steel structures using HMH (Von Mises) plastic criterion with the multilinear kinematic hardening stress-strain relations for the various level of the temperatures and the degradation of the strength were considered. The uncertainty of the input data (Table 3) and the results of the nonlinear analysis of the technological structures for various level of the accident pressure were taken.

The overpressure loads from 250 kPa to 1 000 kPa using the nonlinear solution of the static equilibrium considering the geometric and material nonlinearities of the steel solid and shell layered elements were considered. The recapitulation of the probability of failure calculated by the RSM simulation method is presented in Fig.11 depending on the level of the pressure. The idealized fragility curves of the reactor protective hood are determined analytically for normal distribution with 5% envelope (see Fig.12).

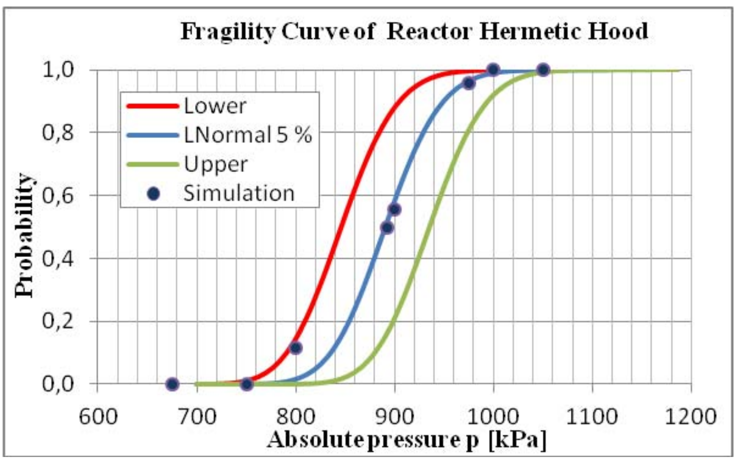


Fig.12: Fragility curves of the reactor protective hood determined analytically for normal distribution with 5% envelope

## 9 CONCLUSIONS

The presented analyses are based on the methodology of the probabilistic analysis of structures of hermetic zone of NPP with reactor VVER44/213 detailed described in work [12]. The nonlinear probabilistic analysis of the reactor cover failure is in accordance with the requirements IAEA [7] and NRC [18 and 19], experiences from the similar analysis NPP in abroad [12 and 22], new knowledges from the probabilistic analysis of structures [2-6, 8-22] and our experiences from the previous analysis [12-15].

These analyses go out from the previous results of the monitoring of material properties and NPP structures, as well as from the results of the resistance analysis of the important structural components from the point of the initiated accidents. The structures were analyzed on impact of the extreme loads situation defined in the scenarios of the internal accidents.

The nonlinear analysis of the loss of the containment integrity was made for the overpressure loads from 250 kPa using the nonlinear solution of the static equilibrium considering the geometric and material nonlinearities of the steel shell and solid elements. The nonlinear analyses were performed in the ANSYS program using the HMH plastic condition [10].

The probability analysis of the loss of the reactor cover integrity was made for the overpressure loads from 250 kPa to 1000 kPa using the nonlinear solution of the static equilibrium. The uncertainties of the loads level (temperature, dead and live loads), the material model of the steel structures as well as the inaccuracy of the calculation model and the numerical methods [12 and 15] were taken into account in the approximation RSM method for CCD experimental design and $10^6$ Monte Carlo simulations.

The critical technology segment of the containment is the reactor protective hood with the failure pressure $p_{u.0.05}$= 766.9 kPa. The mean value of pressure capacity of the reactor protective hood is $p_{u.0.50}$= 891.8 kPa, the 95% upper bound is $p_{u.0.95}$= 973.6 kPa.

### ACKNOWLEDGMENT

The project was performed with the financial support of the Grant Agency of the Slovak Republic (VEGA 1/0265/16).

### LITERATURE

[1] ABRAHAM, ASME Boiler and Pressure Vessel Code, Section III, Div. 1, Appendix F, "Rules for Evaluation of Service Loadings with Level D Service Limits," American Society of Mechanical Engineers, 1998.

[2] ČAJKA, R. & KREJSA, M. Measured Data Processing in Civil Structure Using the DOProC, Method, *Advanced Materials Research* Vol. 859, p. 114-121, DOI 10.4028/ www.scientific.net/ AMR.859.114, December, 2013 .

[3] ENSREG, *Post-Fukushima accident. Action Plan. Follow-up of the peer review of the stress tests performed on European nuclear power plants*, 2012.

[4] GOTTWALD, J. & KALA, Z., Sensitivity analysis of tangential digging forces of the bucket wheel excavator SchRs 1320 for different terraces. *Journal of Civil Engineering and Management*, 18:5, 2012, 609-620, http://dx.doi.org/10.3846/13923730.2012.719836.

[5] HALDAR, A. & MAHADEVAN, S. *Probability, Reliability and Statistical Methods in Engineering Design*, John Wiley & Sons, New York, 2000, ISBN-13: 978-0471331193.

[6] HANBOOK 5. *Implementation of Eurocodes Reliability Backgrounds. Design of Buildings for the Fire Situation.* Development of Skills Facilitating Implementation of Eurocodes. Leonardo Da Vinci Pilot Project CZ/02/B/F/PP-134007. Prague, CR, 10.2005.

[7] IAEA, *Safety Series No. SSG-4, Development and Application of Level 2 Probabilistic Safety Assessment for Nuclear Power Plants*, Vienna, 2010.

[8] JCSS 2011. *JCSS Probabilistic Model Code.* Zurich: Joint Committee on Structural Safety. www.jcss.byg.dtu.dk, 2011.

[9] KALA, Z. Sensitivity analysis of steel plane frames with initial imperfections, Engineering Structures, 33, 2011, pp.2342-2349, ISSN: 0141-0296.

[10] KOHNKE, P. *ANSYS, Theory,* SAS IP Inc. Canonsburg, 2008.

[11] KONEČNÝ, P. BROŽOVSKÝ, J. & KRIVÝ, V. Simulation Based Reliability Assessment Method using Parallel Computing. In *Proceedings of 1st International Conference on Parallel, Distributed and Grid Computing for Engineering, Civil Comp Proceedings*, 2009, issue 90, pp. 542–549 (8 p), ISSN: 1759-3433

[12] KRÁLIK, J. *Safety and Reliability of Nuclear Power Buildings in Slovakia. Earthquake-Impact-Explosion.* Ed. STU Bratislava, 2009, 307pp. ISBN 978-80-227-3112-6.

[13] KRÁLIK, J. *Reliability Analysis of Structures Using Stochastic Finite Element Method,* Ed. STU Bratislava, 2009, 143pp. ISBN 978-80-227-3130-0.

[14] KRÁLIK, J. Probabilistic Safety Analysis of the Nuclear Power Plants in Slovakia. In: *Journal of KONBiN*, Safety and Reliability Systems, Ed. VERSITA Central European Science Publishers, Warszawa, ISSN 1895-8281, No 2, 3 (14, 15) 2010, pp. 35-48.

[15] KRÁLIK, J. et al. Structural Reliability for Containment of VVER 440/213 Type, In *Safety and Reliability: Methodology and Applications - Nowakowski et al.* (Eds) © 2015 Taylor & Francis Group, London, p.2279-2286, ISBN 9781138026810.

[16] KREJSA, M. Probabilistic failure analysis of steel structures exposed to fatigue, In. *Key Engineering Materials*, Vol. 577-578, 2014, Pp. 101-104, ISSN: 1662-9795.

[17] NOVÁK, D. BERGMEISTER, K. PUKL, R. & ČERVENKA, V., Structural assessment and reliability analysis for existing engineering structures, Theoretical background. *Structure and infrastructure engineering*, Vol. 9, No. 2, 2009, pp. 267-275, http://dx.doi.org/10.1080/15732470601185612.

[18] NRC, RG 1.200, *An Approach for Determining the Technical Adequacy of Probabilistic Risk Assessment Results for Risk-Informed Activities*, U.S. Nuclear Regulatory Commission, Washington, DC. 2009.

[19] NUREG/CR-6906, *Containment Integrity Research at Sandia National Laboratories*, An Overview, Sandia National Laboratories, SAND2006-2274P, US NRC Washington, July 2006.

[20] SUCHARDOVÁ, P., BERNATÍK, A. & SUCHARDA, O., 2012. Assessment of loss results by means of multi - Criteria analysis. In: Advances in Safety, Reliability and Risk Management - *Proc. of the European Safety and Reliability Conference, ESREL 2011*. London: CRC Press-Taylor & Francis group, 2011, pp. 1563-1570. ISBN 978-0-415-68379-1.

[21] SÝKORA, M. & HOLICKÝ, M. Assessment of Uncertainties in Mechanical Models, *Applied Mechanics and Materials*, Vol. 378, 2013, pp.13-18, © (2013) Trans Tech Publications, Switzerland, doi:10.4028/www.scientific.net/AMM.378.13.

[22] VEJVODA, S., KERŠNER, Z., NOVÁK, D. & TEPLÝ, B. Probabilistic Safety Assessment of the Steam Generator Cover, In *Proc. of the 17th International Conference on Structural Mechanics in Reactor Technology* (SMiRT 17), Prague, Czech Republic, August 17-22, 2003, in CD, M04-4, 10 pp.